Semiflexible polymers under external fields confined to two dimensions

A. Lamura[1, a)] and R. G. Winkler[2, b)]

[1)]*Istituto Applicazioni Calcolo, CNR, Via Amendola 122/D, 70126 Bari, Italy*

[2)]*Theoretical Soft Matter and Biophysics, Institute for Advanced Simulation, Forschungszentrum Jülich, 52428 Jülich, Germany*

(Dated: 30 November 2012)

The non-equilibrium structural and dynamical properties of semiflexible polymers confined to two dimensions are investigated by molecular dynamics simulations. Three different scenarios are considered: The force-extension relation of tethered polymers, the relaxation of an initially stretched semiflexible polymer, and semiflexible polymers under shear flow. We find quantitative agreement with theoretical predictions for the force-extension relation and the time dependence of the entropically contracting polymer. The semiflexible polymers under shear flow exhibit significant conformational changes at large shear rates, where less stiff polymers are extended by the flow, whereas rather stiff polymers are contracted. In addition, the polymers are aligned by the flow, thereby the two-dimensional semiflexible polymers behave similarly to flexible polymers in three dimensions. The tumbling times display a power-law dependence at high shear rate rates with an exponent comparable to the one of flexible polymers in three-dimensional systems.

[a)]a.lamura@ba.iac.cnr.it

[b)]r.winkler@fz-juelich.de

I. INTRODUCTION

Semiflexibility is a characteristic property of a broad range of biological polymers. Prominent examples are DNA, filamentous actin, microtubules, or viruses such as fd-viruses[1–5]. The rigidity is fundamental for their biological functions. For example, the DNA persistence length strongly affects its packing in the genome or inside a virus capsid. Actin filaments are an integral part of the cytoskeleton and their rigidity determines its particular mechanical properties. Hence, considerable effort has been devoted to unravel the mechanical and dynamical properties of semiflexible polymers[4,6–18].

Advances in single-molecule spectroscopy prompted experimental and theoretical studies of non-equilibrium properties of semiflexible polymers[19–26]. Fluorescence microscopy studies on single DNA molecules in shear flow reveal large conformational changes and an intriguing dynamics, denoted as tumbling motion[23–26]. This implies specific non-equilibrium conformational, dynamical, and rheological properties, which have been analyzed experimentally[24–30], theoretically[31–49], and by computer simulations[25,50–71].

These studies typically consider semiflexible polymers in three-dimensional space. Much less attention has been payed to polymers in two dimensions, although we may expect to see particular features in their equilibrium and non-equilibrium dynamical properties. Two-dimensional behavior is realized for strongly adsorbed polymers at, e.g., a solid surface, a membrane, or at the interface between immiscible fluids. Experiments reveal a strong dependence of the diffusive dynamics of adsorbed polymers on the underlaying substrate[72,73]. Moreover, theoretical and simulation studies predict a strongly correlated dynamics in two-dimensional polymer melts[74]. Little is known about the non-equilibrium properties of polymers in two dimensions. Here, we refer to recent simulation studies of end-tethered semiflexible polymers, where the central monomer is periodically excited[75,76]. These simulations find a crossover from a limit cycle to an aperiodic dynamics with increasing stiffness.

There are two major differences to three-dimensional systems. First of all, excluded volume interactions play a more pronounced role. The non-crossability leads, e.g., to a segregation of polymers in two dimensions[74]. We expect a strong impact of these interactions on non-equilibrium properties too. Secondly, hydrodynamic interactions can be neglected under certain circumstances[77]. This applies to strongly adsorbed polymers, where the polymer-substrate interaction dominates the dynamics of the polymer. It is certainly not appropriate

for polymers confined at fluid-fluid interfaces.

In this article we investigate the non-equilibrium structural and dynamical properties of semiflexible polymers by computer simulations. As discussed above, we assume that the local polymer friction is determined by its interaction with the substrate and, hence, neglect hydrodynamics. Thus, we exploit the Brownian multiparticle collision (B-MPC) dynamics approach described in Refs. 78–80. By varying the chain stiffness, we gain insight into the dependence of the polymer properties on stiffness. Moreover, by comparison with existent results on three-dimensional systems, we uncover specific effects of the reduced dimensionality.

Three different situations are considered. We briefly touch the force-extension relation of a semiflexible polymer and show that it is well described by theory[3,14]. In addition, we examine the end-to-end vector relaxation behavior of initially stretched polymers. We find excellent agreement with the power-law dependence obtained in experiments[77]. This suggests that our model is a useful coarse-grained representation of a DNA molecule, at least for the considered properties. The major focus of the paper is on the non-equilibrium properties of semiflexible polymers under shear flow. We discuss a broad range of structural and dynamical quantities and stress the universal character and/or their particular, two-dimensional features.

The paper is organized as follows. In Sec. II the polymer model is described and the simulation method is introduced. In Sec. III the force-extension relation of a tethered polymer in a uniform external field is discussed. Section IV presents results on the time dependent relaxation behavior of a stretched semiflexible polymer. The structural properties of free polymers under shear flow are discussed in Sec. V, and their tumbling dynamics is analyzed in Sec. VI. Finally, Sec. VII summarizes our findings.

II. MODEL AND METHOD

The polymer is modeled as a linear chain composed of N beads of mass M. Its intramolecular interactions are described by the potential $U = U_{bond} + U_{bend} + U_{ex}$. Successive beads are linked by the harmonic bond potential

$$U_{bond} = \frac{\kappa_h}{2} \sum_{i=1}^{N-1} (|\boldsymbol{r}_{i+1} - \boldsymbol{r}_i| - r_0)^2, \tag{1}$$

where $\boldsymbol{r}_i$ is the position vector of bead i $(i = 1, \ldots, N)$, κ_h is the spring constant, and r_0 the bond length. The bond bending potential

$$U_{bend} = \kappa \sum_{i=1}^{N-2} (1 - \cos \varphi_i) \tag{2}$$

accounts for the bending stiffness of the polymer, with κ the bending rigidity and φ_i the angle between two consecutive bond vectors. In the semiflexible limit $\kappa \to \infty$, the bending stiffness is related to the persistence length by $L_p = 2\kappa r_0/k_B T$, where $k_B T$ is the thermal energy, with T the temperature and k_B Boltzmann's constant. Excluded-volume interactions are ensured by the shifted and truncated Lennard-Jones potential

$$U_{ex} = 4\epsilon \left[\left(\frac{\sigma}{r}\right)^{12} - \left(\frac{\sigma}{r}\right)^6 + \frac{1}{4} \right] \Theta(2^{1/6}\sigma - r), \tag{3}$$

where r denotes the distance between two non-bonded beads and $\Theta(r)$ is the Heaviside function ($\Theta(r) = 0$ for $r < 0$ and $\Theta(r) = 1$ for $r \geq 0$). The dynamics of the beads is described by Newton's equations of motion, which we integrated by the velocity-Verlet algorithm with time step Δt_p[81,82].

The polymer is coupled to a Brownian heat bath, which we implement via the B-MPC approach[78,79,83]. Hence, no hydrodynamic interactions are taken into account. In B-MPC, a bead performs stochastic collisions with a phantom particle which mimics a fluid element of a certain size. The momentum of the phantom particle is taken from a Maxwell-Boltzmann distribution of variance $M k_B T$ and mean given by the average momentum of the fluid field, which is zero at rest or $(M\dot{\gamma} y_i, 0)^T$ in the case of an imposed shear flow of shear rate $\dot{\gamma}$ in the xy−plane. For the stochastic process itself, we apply the stochastic rotation dynamics realization of the MPC method[79,84,85]. Here, the relative velocity of a polymer bead, with respect to the center-of-mass velocity of the bead and the associated phantom particle, is rotated in the xy−plane by angles $\pm\alpha$. The time interval between collisional interactions is Δt, which is larger than the time step Δt_p.

The simulations are performed for the parameters $\alpha = 130^o$, $\Delta t = 0.1 t_u$, where the time unit is $t_u = \sqrt{m r_0^2/(k_B T)}$, $M = 5m$, $\kappa_h r_0^2/(k_B T) = 4 \times 10^3$, $\epsilon/(k_B T) = 1$, $\sigma = r_0$, $N = 51$ so that polymer length is $L = 50 r_0$, and $\Delta t_p = 10^{-2} \Delta t$. With this choice for κ_h, the length of the polymer is kept constant within 1% for all systems.
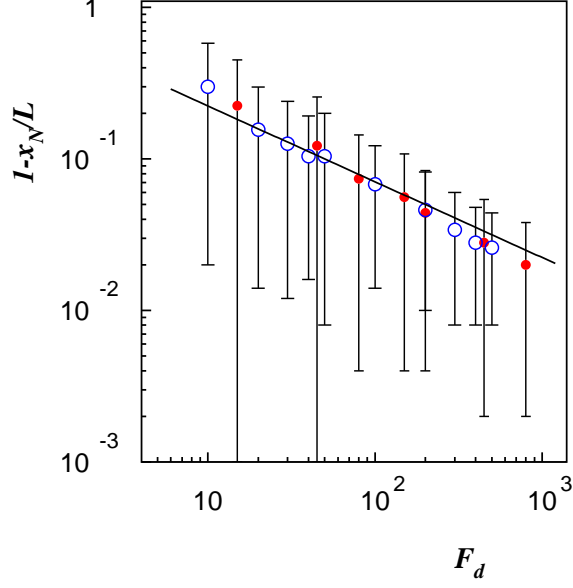
FIG. 1. Polymer extension along the direction of the external force for the persistence lengths $L_p/L = 2(\circ)$, $4(\bullet)$ as a function of the dimensionless force $F_d = L_pF(N-1)/(k_BT)$. The full line represents Eq. (4) and has the slope $-1/2$.

III. POLYMER FORCE-EXTENSION RELATION IN UNIFORM FIELD

We consider a single tethered polymer with its endpoint $\boldsymbol{r}_1$ fixed at $\boldsymbol{r}_1 = 0$ without additional restrictions on the orientation of the first bond. Every monomer is subjected to the external force F along the x-direction of the Cartesian reference frame, e.g., due to an external electric field E_x, where the force is $F = qE_x$, with q the electric charge of the monomer. As is well known, the polymer is stretched along the force direction, where the extension increases non-linearly with increasing force[86,87]. Theoretical calculations based on the Kratky-Porod[88] wormlike chain model predict the asymptotic dependence

$$\frac{x_N}{L} = 1 - \left(\frac{k_BT}{2L_pF(N-1)}\right)^{1/2} \tag{4}$$

for $|x_N| \to L$.

Simulation results are presented in Fig. 1 for the persistence lengths $L_p/L = 2, 4$. They agree very well with the theoretical prediction (4). This confirms that the model represents a continuous semiflexible polymer over the presented range of forces. Due to the discrete nature of the model, deviations will appear from the predictions of continuous semiflexible polymers[3,14,87,89] for large forces, as shown in Refs. 86, 90, and 91, and a crossover will occur
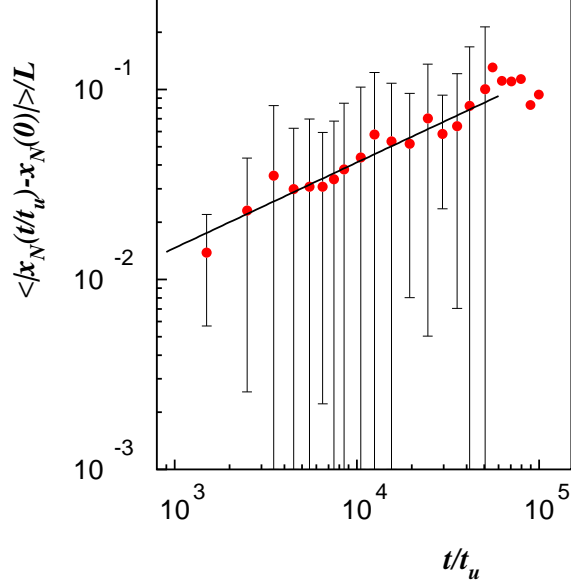
FIG. 2. Relaxation of the end-to-end distance along the stretching direction $|x_N(t/t_u) - x_N(0)|$ of a semiflexible polymer with $L_p/L = 2$. The line indicates a fit in the time range $t/t_u = 10^3 - 50 \times 10^3$ and has the slope 0.45.

from the force-extension relation of a semiflexible model to that of a freely jointed chain. The effects of attractive interactions between non consecutive nearest neighbor beads[91] on the described picture might be interesting to be investigated in the future.

IV. RELAXATION OF STRETCHED POLYMER

Releasing the force on a stretched polymer leads to its collapse into an equilibrium conformational state. This relaxation exhibits a characteristic time dependence. Figure 2 displays the relaxation behavior of the x-component of the end-to-end vector of a stretched semiflexible polymer. The initial average stretching along the $x-$direction is $x_N(0)/L = 0.945$, induced by the force $FL_p(N-1)/(k_BT) = 200$. We observe a power-law decrease of the extension according to $|x_N(t) - x_N(0)|/L \sim t^\gamma$ over a broad time scale. A fit of the data, which are averages over 20 independent realizations, yields the exponent $\gamma = 0.45 \pm 0.03$. This value is in remarkable agreement with the exponent 0.46 ± 0.08 found in two-dimensional experiments[77].

6

V. SEMIFLEXIBLE POLYMER UNDER SHEAR FLOW

In our study of semiflexible polymers under shear flow in two-dimensional space, we consider the persistence lengths $L_p/L = 0.1, 0.4, 2, 10$. The corresponding equilibrium end-to-end vector relaxation times are $\tau_0/t_u \simeq (161, 370, 676, \text{ and } 707) \times 10^3$, respectively. The strength of the flow is characterized by the Weissenberg number $Wi = \dot{\gamma}\tau_0$ in the range $1 \leq Wi \leq 800$.

A. Conformational Properties

1. End-to-End Vector

Probability distribution functions (PDFs) of the polymer end-to-end distance $R_e = |\boldsymbol{r}_N - \boldsymbol{r}_1|$ are presented in Fig. 3 for the Weissenberg numbers $Wi = 8, 80, 800$ and the various persistence lengths. As shown in Fig. 3(a), for small persistence lengths, the polymers are able to assume coil-like conformations, which give nearly constant PDFs over a wide range of end-to-end distances. Very small distances are suppressed by excluded-volume interactions and large distances are rarely sampled due to entropic penalties. However, larger shear rates lead to a sampling of large R_e values. At low shear rates, an increasing persistence length naturally leads to a preference of large R_e values. Shear, however, leads to an opposite behavior. At a given L_p/L, an increasing shear rate gives rise to an increase in the probability distribution at smaller end-to-end distances. The effect becomes more pronounced for larger stiffnesses (cf. Fig. 3 (c) and (d)). This is in agreement with the predictions of Ref. 49 that semiflexible polymers under shear flow behave more and more like flexible polymers with increasing Weissenberg number.

Figure 4 displays the mean end-to-end distances as function of Wi. For every shear rate, $\langle R_e \rangle$ is smaller for the more flexible polymer. However, $\langle R_e \rangle$ increases for flexible polymers, whereas it decreases for the stiffer ones. As predicted by theory[49], we expect that the end-to-end distances become similar for all stiffnesses in the asymptotic limit $Wi \to \infty$. As the figure clearly reveals, in the stationary non-equilibrium state, a semiflexible polymer is never fully stretched. This has also been observed in simulations of flexible polymers[69,70] and in experiments on DNA molecules[25,28].

Mean square end-to-end distances $\langle R_{ex}^2 \rangle$ along the flow direction are displayed in Fig. 5.
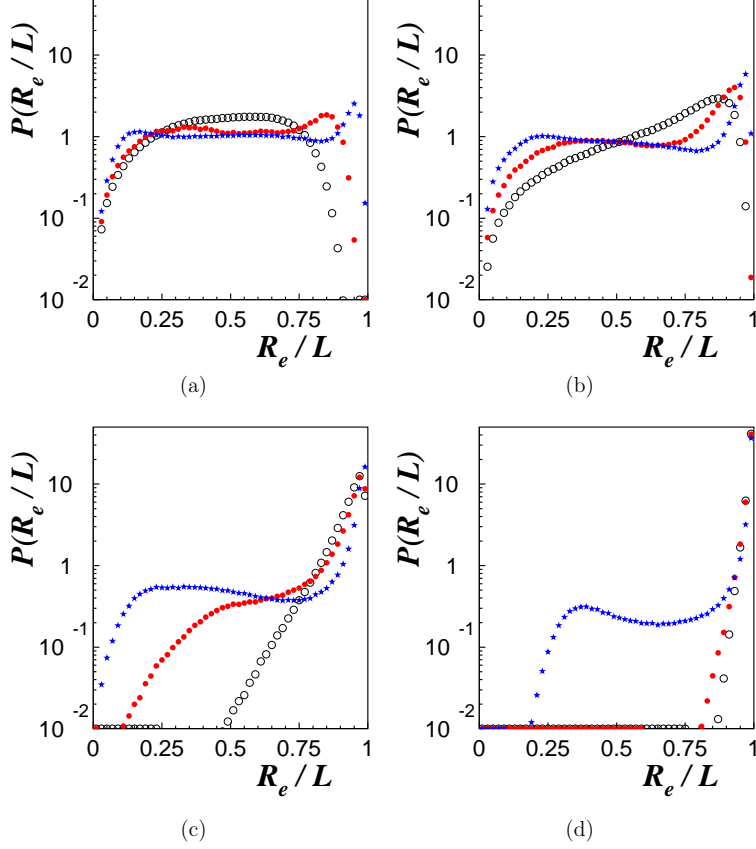
FIG. 3. Probability distributions of the polymer end-to-end distance $R_e = |\mathbf{r}_N - \mathbf{r}_1|$ for the Weissenberg numbers $Wi = 8(\circ)$, $80(\bullet)$, and $800(\star)$ and $L_p/L = 0.1(a)$, $0.4(b)$, $2(c)$, $10(d)$.

They also show that semiflexible polymers are never fully stretched. Moreover, the various curves reveal a very weak persistence length dependence for polymers with $L_p/L \gtrsim 0.4$. They closely follow the same Weissenberg number dependence. This has been predicted in Ref. 49 and is related to the fact that the rather stiff polymers become first aligned with the flow at moderate shear rates. Only at larger shear rates, deformation sets in. This is also evident from Fig. 4, which clearly exhibits a dependence of the "critical" Weissenberg number on the persistence length, above which $\langle R_e \rangle$ decreases with increasing shear rate. Below the critical value, the polymers are aligned by the flow and above, in addition, they are deformed[49].

In Fig. 6 mean square end-to-end distances $\left\langle R_{ey}^2 \right\rangle$ are shown along the gradient direction. The polymers of the various stiffnesses shrink transverse to the flow direction. Thereby, we observe a slight dependence on persistence length over the considered range. The decay
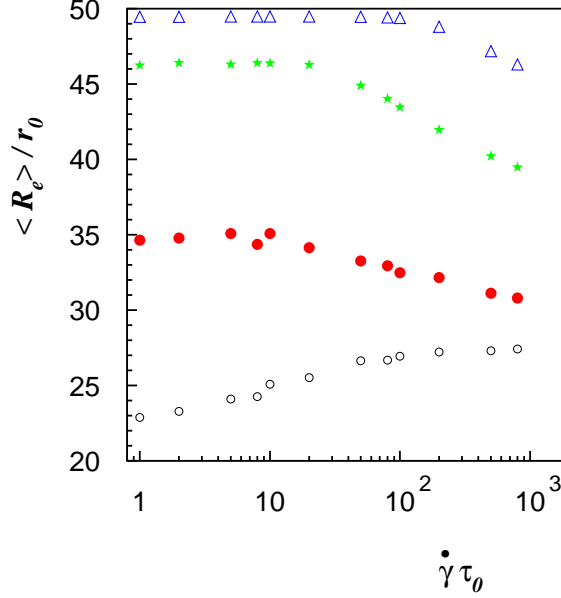
8

FIG. 4. Mean values $\langle R_e \rangle$ of the end-to-end distance as function of the Weissenberg number for the persistence lengths $L_p/L = 0.1 (\circ)$, $0.4 (\bullet)$, $2 (\star)$, and $10 (\triangle)$.

at larger Wi can approximately be described by the power-law $\langle R_{ey}^2 \rangle \sim Wi^{-\nu}$, with $\nu \approx 1/2$. This dependence is consistent with the decay of the radius-of-gyration tensor of three-dimensional systems[28,52,69]. However, theoretically an exponent $\nu = 2/3$ is expected[17,49], which seems to be reached for much higher Weissenberg numbers in Ref. 25. Hence, the exponent $\nu = 1/2$ could characterize a crossover behavior only.

2. Bond Angle

To further characterize the polymer conformational properties, we present in Fig. 7 the average bond angles $\langle \varphi_i \rangle$ (2) between successive bond vectors along the semiflexible polymers. As expected, the angles $\langle \varphi_i \rangle$ decrease with increasing persistence length and are close to zero for $L_p/L = 10$. At small persistence lengths, the values of $\langle \varphi_i \rangle$ decrease with increasing shear rate, specifically toward the middle of the chain, due to polymer stretching by the flow. The situation is reverted at large persistence lengths, where the angles $\langle \varphi_i \rangle$ increase with the shear rate.
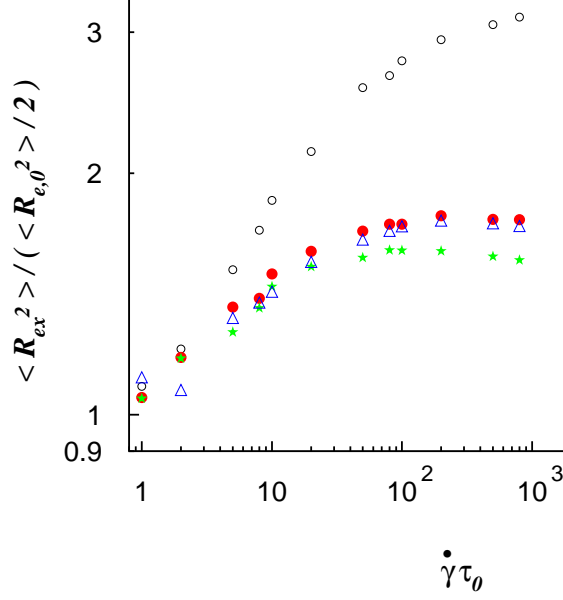
FIG. 5. Mean square end-to-end distances along the flow direction as function of the Weissenberg number for the persistence lengths $L_p/L = 0.1(\circ)$, $0.4(\bullet)$, $2(\star)$, and $10(\triangle)$. $\langle R_{e,0}^2 \rangle$ is the mean square end-to-end distance at equilibrium.

Average bond angles

$$\langle \varphi \rangle = \frac{1}{N-2} \sum_{i=1}^{N-2} \langle \varphi_i \rangle \tag{5}$$

are displayed in Fig. 8 as function of Weissenberg number and for various persistence lengths. Evidently, the mean values are independent of shear rate for the larger persistence lengths. Only for the considered most flexible polymer a decrease of $\langle \varphi \rangle$ is found as already expected from Fig. 7.

This minor change in the bond-bond orientational behavior is surprising in the light of the decreasing mean end-to-end distance (cf. Fig. 4). This is explained on the one hand by the nearly rigid rod-like rotation of the semiflexible polymers at lower Weissenberg numbers and on the other hand by the formation of U-shaped conformations with only small and local bending of the polymer, as reflected in Fig. 7(c) and (d) at higher values of Wi. Typical conformations of stiff polymers at low and high Weissenberg numbers are presented in Fig. 9 (see also the movies in the supplementary material[92]).
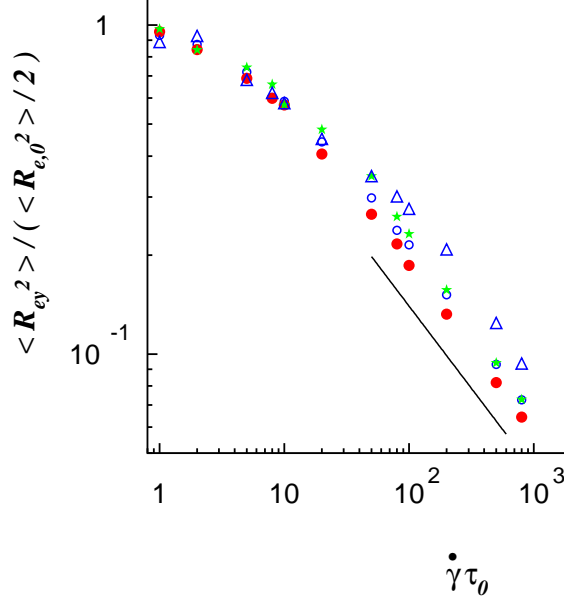
10

FIG. 6. Mean square end-to-end distances along the gradient direction as function of the Weissenberg number for the persistence lengths $L_p/L = 0.1(\circ)$, $0.4(\bullet)$, $2(\star)$, and $10(\triangle)$. The full line has the slope $-1/2$. $\langle R_{e,0}^2 \rangle$ is the mean square end-to-end distance at equilibrium.

B. Alignment

Polymers under flow are not only deformed, but also exhibit a preferred, flow induced orientation[25,28,49,64,69,70]. To characterize the degree of alignment, we calculate the probability distribution of the angle ϕ between the end-to-end vector and the flow direction. Examples are shown in Fig. 10 for various Weissenberg numbers and persistence lengths. There is no preferred angle at equilibrium. With increasing shear rate, the distribution function exhibits a maximum at a non-zero, positive value ϕ_m. This maximum shifts to smaller values with increasing shear rate. At the same time the distribution function becomes narrower. The latter implies that a polymer aligns preferentially in a particular direction and samples other angles only rarely.

Interestingly, the probability distribution functions become asymmetric with increasing shear rate and exhibit a second maximum at large angles. Thereby, the second maximum moves to larger angles with increasing stiffness. The strong asymmetry, particular for lower Weissenberg numbers, seems to be specific for two-dimensional systems, because (flexible) polymers in three dimensions[70] exhibit more symmetric distributions. The second
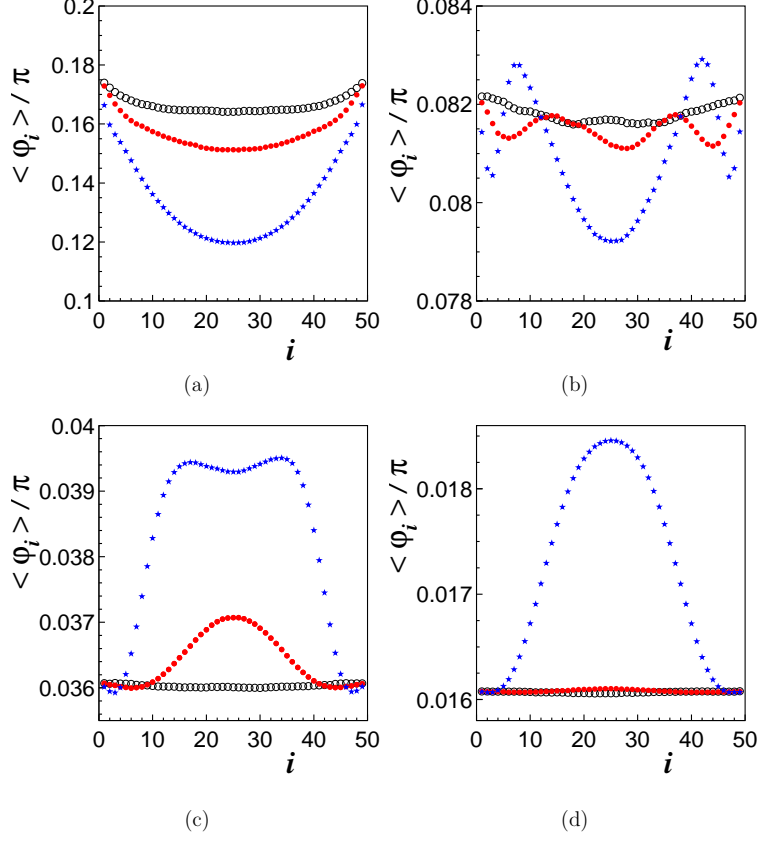
11

FIG. 7. Average local bond angle $\langle \varphi_i \rangle$ along the polymer contour for the Weissenberg numbers $Wi = 8(\circ)$, 80, ($\bullet$), and $800(\star)$ and the persistence lengths $L_p/L = 0.1(a)$, $0.4(b)$, $2(c)$, and $10(d)$.

peak is peculiar for rather stiff polymers. However, it is not clear whether it appears in two-dimensional systems only. Here, studies of three-dimensional semiflexible polymers are required to resolve the issue. We report for completeness the fact that the appearance of two peaks in $P(\phi)$ at finite values, symmetric with respect to $\phi = 0$, was observed for two-dimensional grafted polymers with the first bond fixed along the x-direction and $L_p \simeq L$ under equilibrium conditions.[93]

As shown in Fig. 11, the probability distribution functions depend only weakly on the persistence length for Weissenberg numbers $Wi \lesssim 10^2$. In particular, the position of the maximum is virtually independent of L_p.

Figure 12 displays the angles ϕ_m of the central maximum of $P(\phi)$. For small Weissenberg numbers $Wi < 10$, $\tan(2\phi_m)$ decreases as Wi^{-1}, whereas for larger Weissenberg numbers the dependence $\tan(2\phi_m) \sim Wi^{-1/3}$ is obtained. A similar dependence is found for flexible
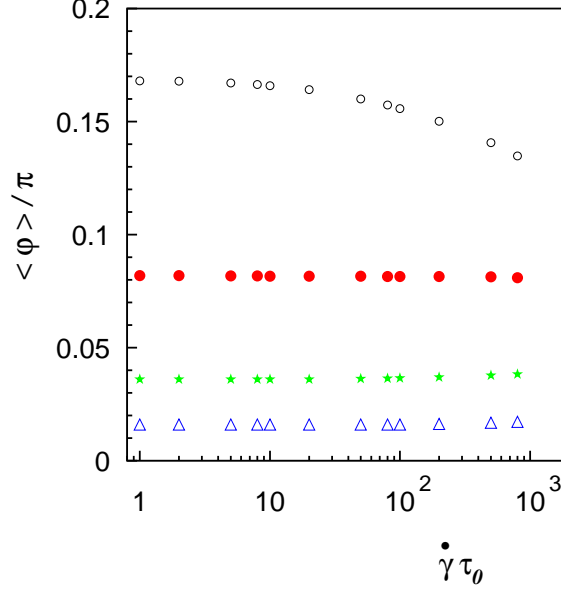
FIG. 8. Average bond angles $\langle \varphi \rangle$ (5) as function of the Weissenberg number for the persistence lengths $L_p/L = 0.1(\circ)$, $0.4(\bullet)$, $2(\star)$, and $10(\triangle)$.

polymers in three dimensions[70] and is predicted theoretically[17,49] independent of dimension. As already suggested by Fig. 11, nearly the same degree of alignment is obtained independent of stiffnesses. However, the values of $\tan(2\phi_m)$ are somewhat smaller for the more flexible polymers in the range $Wi > 10$, as predicted theoretically[49].

Similarly, the width $\Delta\phi$, which is defined as the full width at half maximum of the distribution function $P(\phi)$, decreases as $\Delta\phi \sim Wi^{-1/3}$ at high shear rates. This has also been observed in experiments[26] and predicted theoretically[17].

VI.   TUMBLING DYNAMICS

As mentioned in the Introduction, polymers in shear flow undergo a tumbling motion. A characteristic tumbling time can be obtained from the distribution function $P(t)$ of times between successive zeros of the end-to-end vector component $R_{ex}(t)$ along the flow direction. This distribution exhibits the exponential decay $P(t) \sim \exp\left(-t/\tau_\phi\right)$ at large times, from which the tumbling time τ_ϕ is extracted. Normalized tumbling frequencies $\sim 1/\tau_\phi$ are depicted in Fig. 13, where the full line has slope 2/3.

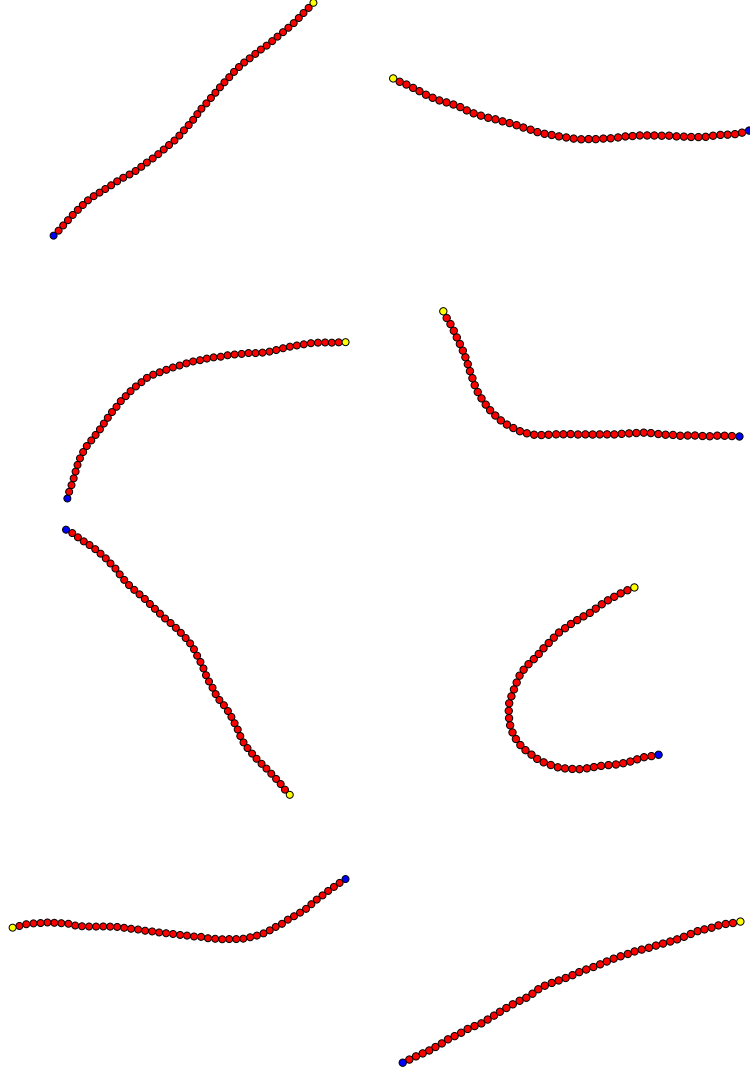As for a three-dimensional system, we obtain $\tau_\phi \sim Wi^{-2/3}$ for the shear rate dependence

FIG. 9. Typical conformations at consecutive times (from top to bottom) of a semiflexible polymer $(L_p/L = 10)$ at $Wi = 8$ (left panel) and $Wi = 800$ (right panel).

of the tumbling times. This confirms that the tumbling times of semiflexible polymers exhibit the same asymptotic Weissenberg number dependence as flexible polymers. Moreover, two-dimensional tumbling behavior seems to be similar to three-dimensional one for semiflexible polymers.

Interestingly, the frequencies for the larger persistence lengths seem to exhibit a fast, rather abrupt increase in the vicinity of $Wi \approx 10$ and approach the dependence $Wi^{2/3}$ for large Weissenberg numbers only. Such a dependence has not been observed in three dimensions so far nor be predicted theoretically. Whether this is a specific two-dimensional
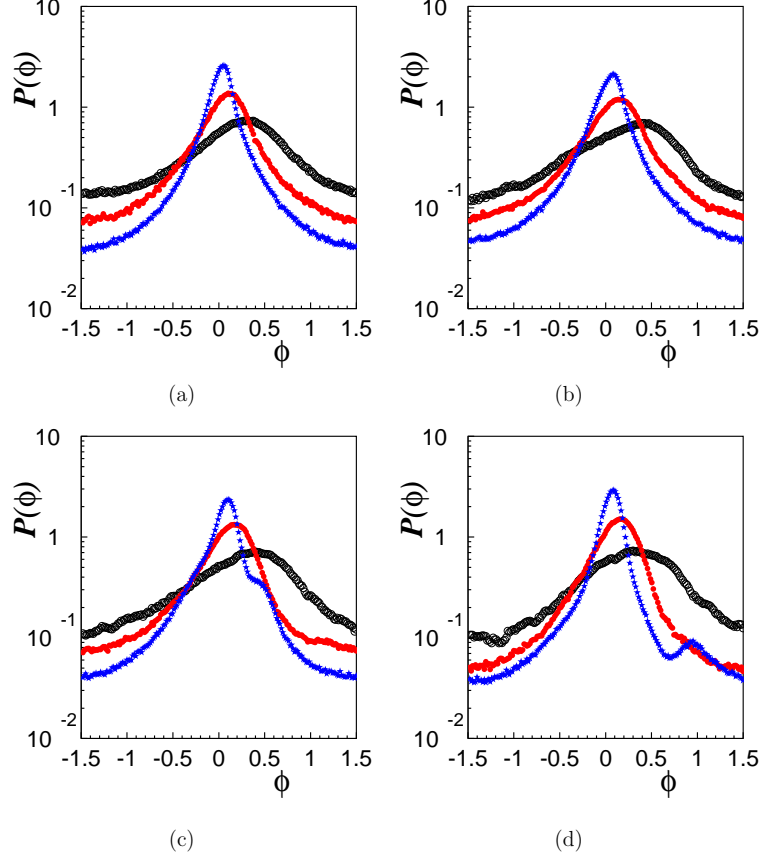
FIG. 10. Probability distributions of the angle ϕ for the Weissenberg numbers $Wi = 8(\circ)$, $80(\bullet)$, and $800(\star)$ and the persistence lengths $L_p/L = 0.1(a)$, $0.4(b)$, $2(c)$, and $10(d)$.
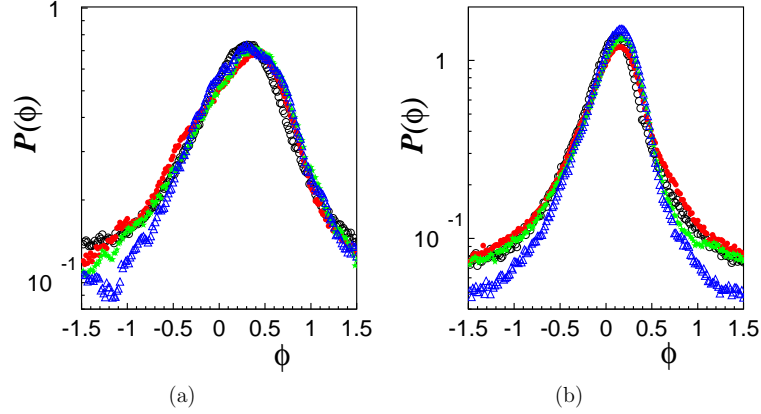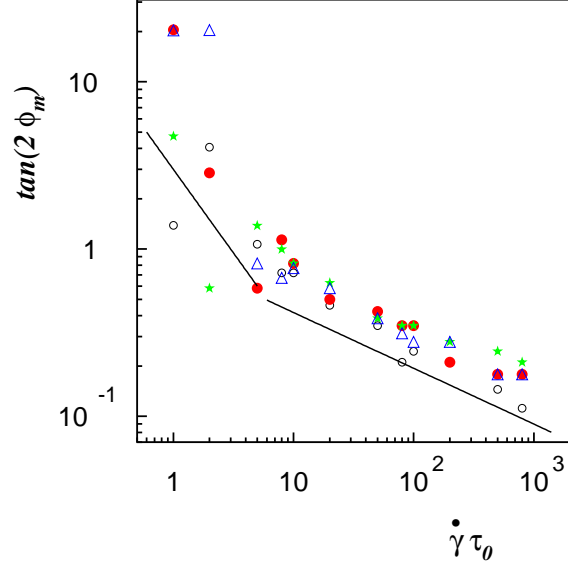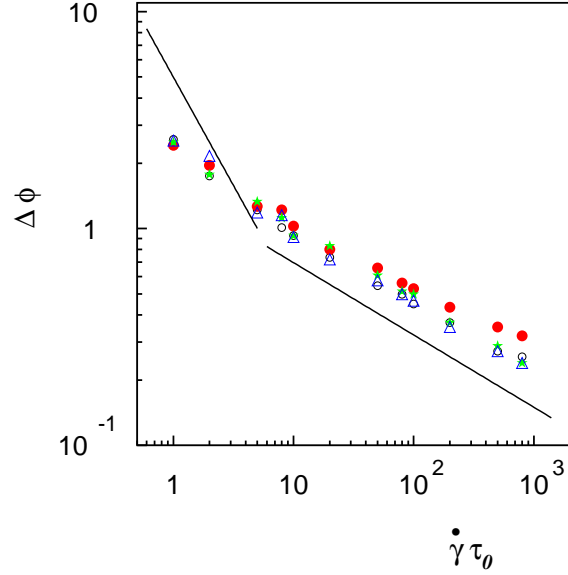

FIG. 11. Probability distributions of the angle ϕ for the Weissenberg numbers $Wi = 8$ (a) and 80 (b) and the persistence lengths $L_p/L = 0.1(\circ)$, $0.4(\bullet)$, $2(\star)$, and $10(\triangle)$.

15

FIG. 12. (a) Angles ϕ_m of the maximum and (b) width $\Delta\phi$ of the distribution function $P(\phi)$ as function of the Weissenberg number for the persistence lengths $L_p/L = 0.1(\circ)$, $0.4(\bullet)$, $2(\star)$, and $10(\triangle)$. The slopes of the full lines are -1 and $-1/3$, respectively.

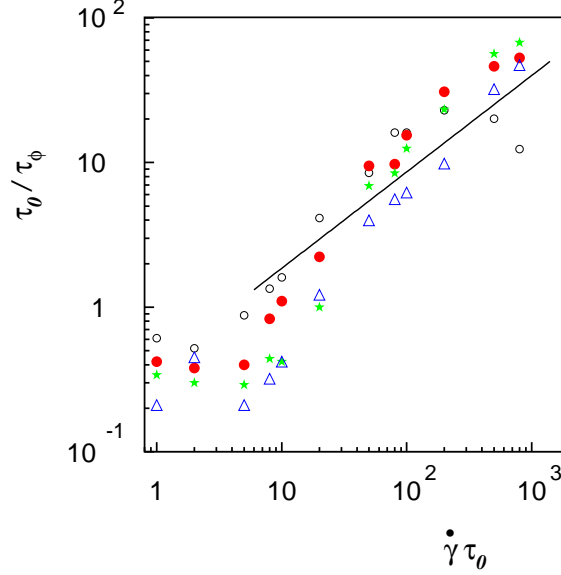features needs to be addressed by simulations of semiflexible polymers in three dimensions.

FIG. 13. Normalized tumbling frequencies τ_0/τ_ϕ as function of the Weissenberg number for the persistence lengths $L_p/L = 0.1(\circ)$, $0.4(\bullet)$, $2(\star)$, and $10(\triangle)$. The line has the slope 2/3.

VII. CONCLUSIONS

We have presented results for the non-equilibrium structural and dynamical properties of semiflexible polymers confined to two dimensions. The analysis of the force-extension relation of a semiflexible polymer in a uniform external field yields excellent agreement with theoretical predictions[86,87] and confirms that the applied model is very well suited to describe semiflexible polymers. Our studies of the end-to-end distance relaxation behavior of initially stretched semiflexible polymers confirm the experimentally obtained power-law time dependence t^γ with the exponent $\gamma = 0.45$, which is in close agreement with the scaling prediction $\gamma = 1/2$ of Ref. 77.

We have also studied the conformation properties of semiflexible polymers under shear flow. We clearly find strong shear-induced conformational changes. Beyond a stiffness dependent Weissenberg number, the average polymer extension decreases with increasing shear rate, in contrast to flexible polymers, where the extension increases. Visual inspection shows that U-shaped conformations appear. Such conformations have also been observed for semi-flexible polymers in microchannel flows, both experimentally[94] and in simulations[95,96]. This confirms that the end-to-end distances become similar in the asymptotic limit of infinite shear rate independent of the stiffness[49]. As for flexible polymers in three dimensions, the

17

semiflexible polymers preferentially align along the flow direction. However, the distribution functions of the end-to-end vector alignment angle are clearly more asymmetric at low Weissenberg numbers than for flexible polymers and exhibit a second peak for large stiffnesses. It is not evident whether these effects are caused by stiffness or confinement to two dimensions. Further simulation studies are necessary to resolve this question.

We have also shown that semiflexible polymers exhibit a tumbling motion, where the tumbling times approximately show the dependence $\tau_\phi \sim Wi^{-2/3}$ on shear rate. Hence, semiflexible polymers reveal in essence the same tumbling behavior as flexible polymers[25,28,47,49,68,70,71,97] and rods[48,49].

There are various aspects, e.g., the appearance of a second peak in the orientational distribution functions and their asymmetry at low shear rates, which need further investigations to clarify the underlaying mechanism. This requires theoretical calculations and/or simulations in two and three dimensions. We hope that our results will stimulate such theoretical studies as well as experimental investigations and will be valuable in the respective endeavors.

REFERENCES

[1] P. Janmey, in *Handbook of Biological Physics*, Vol. 1A (North Holland, Amsterdam, 1995).

[2] C. Bustamante, J. F. Marko, E. D. Siggia, and S. Smith, Science **265**, 1599 (1994).

[3] J. F. Marko and E. D. Siggia, Macromolecules **28**, 8759 (1995).

[4] J. Wilhelm and E. Frey, Phys. Rev. Lett. **77**, 2581 (1996).

[5] M. Ripoll, P. Holmqvist, R. G. Winkler, G. Gompper, J. K. G. Dhont, and M. P. Lettinga, Phys. Rev. Lett. **101**, 168302 (2008).

[6] T. Maeda and S. Fujime, Macromolecules **17**, 2381 (1984).

[7] S. R. Aragón and R. Pecora, Macromolecules **18**, 1868 (1985).

[8] E. Farge and A. C. Maggs, Macromolecules **26**, 5041 (1993).

[9] R. Götter, K. Kroy, E. Frey, M. Bärmann, and E. Sackmann, Macromolecules **29**, 30 (1996).

[10] L. Harnau, R. G. Winkler, and P. Reineker, J. Chem. Phys. **104**, 6355 (1996).

[11] R. Everaers, F. Jülicher, A. Ajdari, and A. C. Maggs, Phys. Rev. Lett. **82**, 3717 (1999).

[12] J. Samuel and S. Sinha, Phys. Rev. E **66**, 050801 (2002).

[13] L. Le Goff, O. Hallatschek, E. Frey, and F. Amblard, Phys. Rev. Lett. **89**, 258101 (2002).

[14] R. G. Winkler, J. Chem. Phys. **118**, 2919 (2003).

[15] G. A. Carria, J. Chem. Phys. **121**, 12112 (2004).

[16] E. P. Petrov, T. Ohrt, R. G. Winkler, and P. Schwille, Phys. Rev. Lett. **97**, 258101 (2006).

[17] R. G. Winkler, S. Keller, and J. O. Rädler, Phys. Rev. E **73**, 041919 (2006).

[18] R. G. Winkler, J. Chem. Phys. **127**, 054904 (2007).

[19] T. T. Perkins, D. E. Smith, R. G. Larson, and S. Chu, Science **268**, 83 (1995).

[20] T. T. Perkins, D. E. Smith, and S. Chu, Science **276**, 2016 (1997).

[21] S. R. Quake, H. Babcock, and S. Chu, Nature **388**, 151 (1997).

[22] R. G. Winkler, Phys. Rev. Lett. **82**, 1843 (1999).

[23] P. LeDuc, C. Haber, G. Boa, and D. Wirtz, Nature **399**, 564 (1999).

[24] D. E. Smith, H. P. Babcock, and S. Chu, Science **283**, 1724 (1999).

[25] C. M. Schroeder, R. E. Teixeira, E. S. G. Shaqfeh, and S. Chu, Phys. Rev. Lett. **95**, 018301 (2005).

[26] S. Gerashchenko and V. Steinberg, Phys. Rev. Lett. **96**, 038304 (2006).

[27] R. E. Teixeira, H. P. Babcock, E. S. G. Shaqfeh, and S. Chu, Macromolecules **38**, 581 (2005).

[28] C. M. Schroeder, R. E. Teixeira, E. S. G. Shaqfeh, and S. Chu, Macromolecules **38**, 1967 (2005).

[29] P. S. Doyle, B. Ladoux, and J.-L. Viovy, Phys. Rev. Lett. **84**, 4769 (2000).

[30] B. Ladoux and P. S. Doyle, Europhys. Lett. **52**, 511 (2000).

[31] J. A. Y. Johnson, Macromolecules **20**, 103 (1987).

[32] W. Bruns and W. Carl, Macromolecules **26**, 557 (1993).

[33] W. Carl and W. Bruns, Macromol. Theory Simul. **3**, 295 (1994).

[34] X. Wang and A. P. Chatterjee, Macromolecules **34**, 1118 (2001).

[35] N. J. Woo and E. S. G. Shaqfeh, J. Chem. Phys. **119**, 2908 (20030).

[36] J. Dubbeldam and F. Redig, J. Stat. Phys. **125**, 225 (2006).

[37] R. B. Bird, C. F. Curtiss, R. C. Armstrong, and O. Hassager, *Dynamics of Polymer Liquids*, Vol. 2 (John Wiley & Sons, New York, 1987).

[38] H. C. Öttinger, *Stochastic Processes in Polymeric Fluids* (Springer, Berlin, 1996).

[39] A. Dua and B. J. Cherayil, J. Chem. Phys. **112**, 8707 (2000).

[40] Y. Rabin and K. Kawasaki, Phys. Rev. Lett. **62**, 2281 (1989).

[41] J. R. Prakash, Macromolecules **34**, 3396 (2001).

[42] S.-Q. Wang, Phys. Rev. A **40**, 2137 (1989).

[43] P. R. Baldwin and E. Helfand, Phys. Rev. A **41**, 6772 (1990).

[44] F. Ganazzoli and G. Raffaini, Macromol. Theory Simul. **8**, 234 (1999).

[45] A. Subbotin, A. Semenov, E. Manias, G. Hadziioannou, and G. ten Brinke, Macro-molecules **28**, 3898 (1995).

[46] R. Prabhakar and J. R. Prakash, J. Rheol. **50**, 561 (2006).

[47] R. G. Winkler, Phys. Rev. Lett. **97**, 128301 (2006).

[48] T. Munk, O. Hallatschek, C. H. Wiggins, and E. Frey, Phys. Rev. E **74**, 041911 (2006).

[49] R. G. Winkler, J. Chem. Phys. **133**, 164905 (2010).

[50] T. Liu, J. Chem. Phys. **90**, 5826 (1989).

[51] A. Celani, A. Puliafito, and K. Turitsyn, Europhys. Lett. **70**, 464 (2005).

[52] J. S. Hur and E. S. G. Shaqfeh, J. Rheol. **44**, 713 (2000).

[53] P. P. Jose and G. Szamel, J. Chem. Phys. **128**, 224910 (2008).

[54] G.-L. He, R. Messina, H. Löwen, A. Kiriy, V. Bocharova, and M. Stamm, Soft Matter **5**, 3014 (2009).

[55] K. D. Knudsen, J. G. de la Torre, and A. Elgsaeter, Polymer **37**, 1317 (1996).

[56] A. V. Lyulin, D. B. Adolf, and G. R. Davies, J. Chem. Phys. **111**, 758 (1999).

[57] R. M. Jendrejack, J. J. de Pablo, and M. D. Graham, J. Chem. Phys. **116**, 7752 (2002).

[58] C.-C. Hsieh and R. G. Larson, J. Rheol. **48**, 995 (2004).

[59] S. Liu, B. Ashok, and M. Muthukumar, Polymer **45**, 1383 (2004).

[60] R. Pamies, M. C. L. Martinez, J. G. H. Cifre, and J. G. de la Torre, Macromolecules **38**, 1371 (2005).

[61] C. Sendner and R. R. Netz, EPL **81**, 54006 (2008).

[62] Y. Zhang, A. Donev, T. Weisgraber, B. J. Alder, M. G. Graham, and J. J. de Pablo, J. Chem. Phys. **130**, 234902 (2009).

[63] C. Pierleoni and J.-P. Ryckaert, Macromolecules **28**, 5097 (1995).

[64] C. Aust, M. Kröger, and S. Hess, Macromolecules **32**, 5660 (1999).

[65] Y. Gratton and G. W. Slater, Eur. Phys. J. E **17**, 455 (2005).

[66] J. F. Ryder and J. M. Yeomans, J. Chem. Phys. **125**, 194906 (2006).

[67] M. Ripoll, R. G. Winkler, and G. Gompper, Phys. Rev. Lett. **96**, 188302 (2006).

[68] H. Kobayashi and R. Yamamoto, Phys. Rev. E **81**, 041807 (2010).

[69] C.-C. Huang, R. G. Winkler, G. Sutmann, and G. Gompper, Macromolecules **43**, 10107 (2010).

[70] C.-C. Huang, G. Sutmann, G. Gompper, and R. G. Winkler, EPL **93**, 54004 (2011).

[71] C.-C. Huang, G. Gompper, and R. G. Winkler, J. Phys.: Condens. Matter **24**, 284131 (2012).

[72] B. Maier and J. O. Rädler, Phys. Rev. Lett. **82**, 1911 (1999).

[73] S. A. Sukhishvili, J. D. Müller, E. Gratton, K. S. Schweizer, and S. Granick, Nature **406**, 146 (2000).

[74] J. P. Wittmer, H. Meyer, A. Johner, T. Kreer, and J. Baschnagel, Phys. Rev. Lett. **105**, 037802 (2010).

[75] A. K. Chattopadhyay and D. Marenduzzo, Phys. Rev. Lett. **98**, 088101 (2007).

[76] Q. Zhang, K. Li, and H. Tang, Int. J. Mod. Phys. B **25**, 1899 (2011).

[77] B. Maier, U. Seifert, and J. O. Rädler, Europhys. Lett. **60**, 622 (2002).

[78] M. Ripoll, R. G. Winkler, and G. Gompper, Eur. Phys. J. E **23**, 349 (2007).

[79] G. Gompper, T. Ihle, D. M. Kroll, and R. G. Winkler, Adv. Polym. Sci. **221**, 1 (2009).

[80] R. G. Winkler, in *Hierarchical Methods for Dynamics in Complex Molecular Systems*, Vol. 10, edited by J. Grotenhorst, G. Sutmann, G. Gompper, and D. Marx (Forschungszentrum Jülich GmbH, Jülich, 2012).

[81] W. C. Swope, H. C. Andersen, P. H. Berens, and K. R. Wilson, J. Chem. Phys. **76**, 637 (1982).

[82] M. P. Allen and D. J. Tildesley, *Computer Simulation of Liquids* (Clarendon Press, Oxford, 1987).

[83] N. Kikuchi, C. M. Pooley, J. F. Ryder, and J. M. Yeomans, J. Chem. Phys. **119**, 6388 (2003).

[84] T. Ihle and D. M. Kroll, Phys. Rev. E **63**, 020201(R) (2001).

[85] A. Lamura, G. Gompper, T. Ihle, and D. M. Kroll, Europhys. Lett. **56**, 319 (2001).

[86] A. Lamura, T. W. Burkhardt, and G. Gompper, Phys. Rev. E **64**, 061801 (2001).

[87] Y. Hori, A. Prasad, and J. Kondev, Phys. Rev. E **75**, 041904 (2007).

[88] O. Kratky and G. Porod, Recl. Trav. Chim. Pays-Bas **68**, 1106 (1949).

[89] T. Odijk, Macromolecules **28**, 7016 (1995).

[90] L. Livadaru, R. R. Netz, and H. J. Kreuzer, Macromolecules **36**, 3732 (2003).

[91] A. Rosa, T. X. Hoang, D. Marenduzzo, and A. Maritan, Macromolecules **36**, 10095 (2003).

[92]See supplementary material at [URL will be inserted by AIP] for movies of a semiflexible polymer ($L_p/L = 10$) at $Wi = 8$ and $Wi = 800$.

[93]G. Lattanzi, T. Munk, and E. Frey, Phys. Rev. E **69**, 021801 (2004).

[94]D. Steinhauser, S. Köster, and T. Pfohl, ACS Macro Letters **1**, 541 (2012).

[95]R. Chelakkot, R. G. Winkler, and G. Gompper, EPL **91**, 14001 (2010).

[96]R. Chelakkot, R. G. Winkler, and G. Gompper, J. Phys.: Condens. Matter **23**, 184117 (2011).

[97]R. Delgado-Buscalioni, Phys. Rev. Lett. **96**, 088303 (2006).